

## Quantifying functional groups in the active layer of polyamide nanofiltration membranes via the dye adsorption method

Li-ping Yue<sup>1</sup>, Fan-xin Kong (✉)<sup>1</sup>, Jin-fu Chen<sup>1</sup>, Ai-guo Zhou<sup>1</sup>,  
and Guang-dong Sun<sup>2</sup>

1 State Key Laboratory of Heavy Oil Processing, Beijing Key Laboratory of Oil & Gas Pollution Control, China University of Petroleum, Beijing 102249, China

2 Research Center for Urban & Rural Water Environmental Technology, China Urban and Rural Holding Group Co., Ltd., Beijing 102249, China

E-mail: kfx11@cup.edu.cn

### 1 R-NH<sub>2</sub> and R-COOH densities

The adsorption behaviors of Orange II and Toluidine Blue O on membrane surfaces are governed by the  $pK_a$  values of R-NH<sub>2</sub> and R-COOH on the membrane surfaces. When the pH value of the solution is lower than the  $pK_a$  value of R-NH<sub>2</sub> (4–5) on the membrane surface, the protonated amine group (R-NH<sub>3</sub><sup>+</sup>) electrostatically adsorbs negatively charged Orange II [1–3]. In contrast, R-NH<sub>3</sub><sup>+</sup> deprotonates and Orange II desorbs from the membrane surface when the solution pH is higher than the  $pK_a$  value of R-NH<sub>2</sub> on the membrane surface. Similarly, when the pH value of the solution is higher than the  $pK_a$  value of R-COOH (6–9) on the membrane surface, the deprotonated carboxyl group (R-COO<sup>-</sup>) electrostatically adsorbs Toluidine Blue O [4]. In contrast, R-COO<sup>-</sup> protonates and Toluidine Blue O desorbs from the membrane surface when the pH value of the solution is lower than the  $pK_a$  value of R-COOH on the membrane surface. The measured dye adsorption/desorption masses of the membrane surface are supposed to be equivalent to the mass of R-NH<sub>3</sub><sup>+</sup> and the mass of R-COO<sup>-</sup>, respectively.

### 2 Detection and quantification limits

The limit of detection (LOD,  $\mu\text{mol}\cdot\text{L}^{-1}$ ) and the limit of quantification (LOQ,  $\mu\text{mol}\cdot\text{L}^{-1}$ ) were calculated based on Eqs. (S1) and (S2), respectively, which are as follows [5]:

$$D = \frac{VC}{S} \quad (\text{S1})$$

$$\text{LOQ} = \frac{10\delta}{k} \quad (\text{S2})$$

where  $\delta$  was standard deviation (SD) of the blank solution without Orange II and Toluidine Blue O, and  $k$  was the slope of the standard curve of Orange II and Toluidine Blue O.  $\delta$  was obtained by measuring the absorbance values of the blank solution at 485 and 630 nm using a UV-Vis spectrophotometer, with the measurement repeated six times.

### 3 UV-Vis spectra and concentration standard curves of Orange II and Toluidine Blue O solution at pH values of 3 and 11

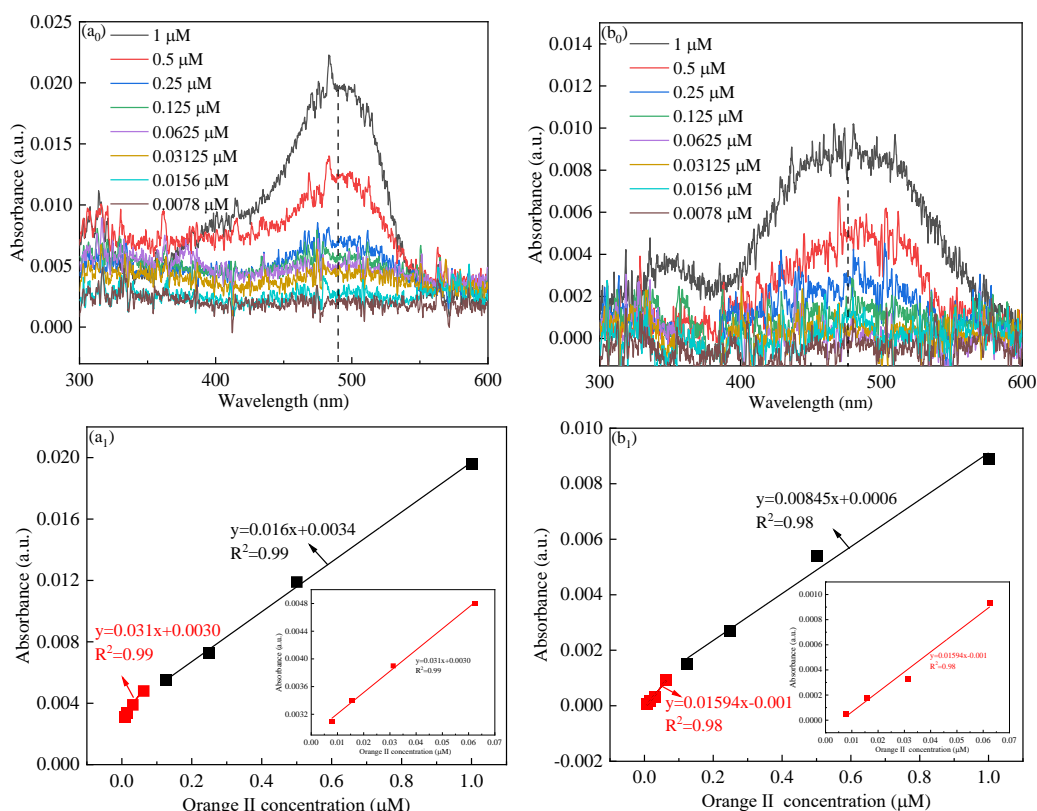


**Fig. S1** UV-Vis spectra (upper) and concentration standard curves (lower) of Orange II solutions at **(a)** pH = 3 and **(b)** pH = 11.

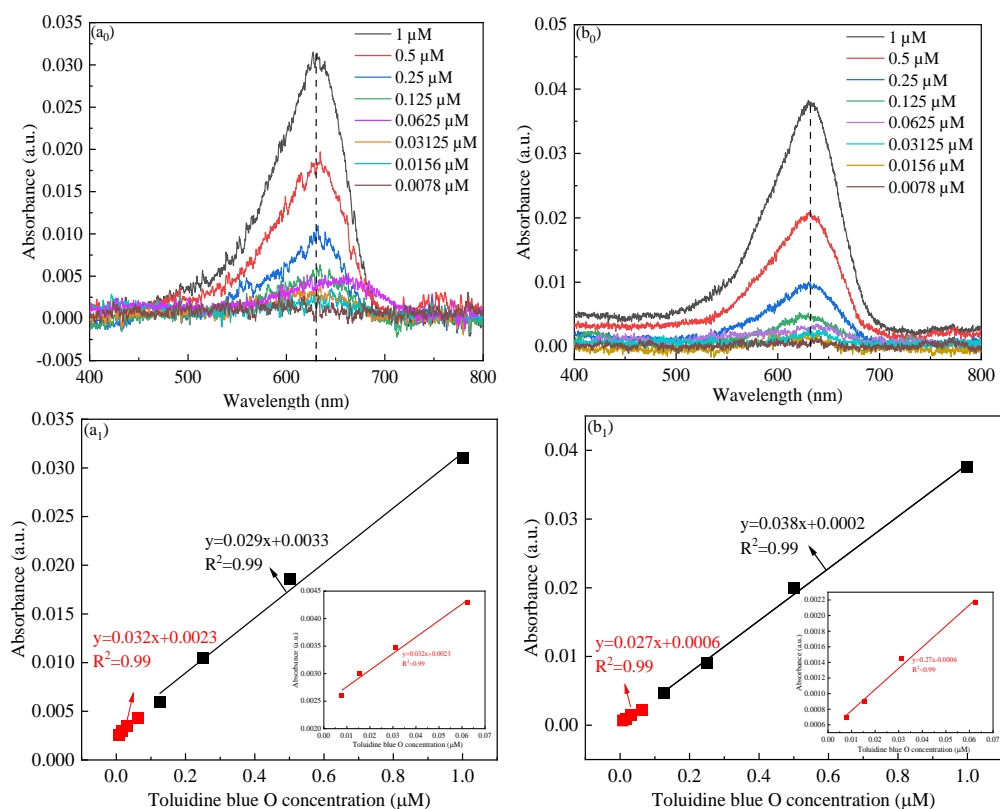


**Fig. S2** UV-Vis spectra (upper) and concentration standard curves (lower) of Toluidine Blue O solutions at **(a)** pH = 3 and **(b)** pH = 11.

As determined using a UV–Vis spectrophotometer, values of the maximum absorption wavelength ( $\lambda_{\max}$ ) for Orange II and Toluidine Blue O were 485 and 630 nm, respectively (Figs. S1 and S2), consistent with those in previous studies [6–7]. A strong linear correlation ( $R^2 > 0.98$ ) was observed between the concentrations of Orange II and Toluidine Blue O and their absorbance within the concentration range of 0.0078–1  $\mu\text{mol}\cdot\text{L}^{-1}$  (Figs. S1 and S2). Thus, the concentrations of Orange II and Toluidine Blue O can be quantified using these standard curves. The densities of  $\text{R-NH}_3^+$  and  $\text{R-COO}^-$  could be determined through quantifying the concentrations of bound Orange II and Toluidine Blue O.

#### 4 R-COOH density on the six membranes surfaces measured via the dye desorption method with and without NaCl

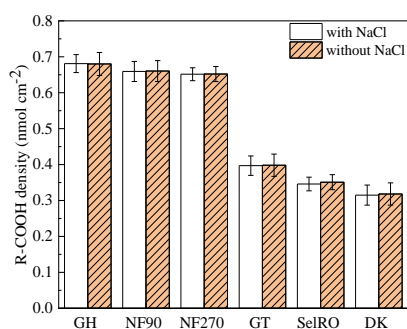


**Fig. S3** Densities of R-COOH on surfaces of six membranes measured using the dye desorption method with and without NaCl.

#### 5 The stability of DK, SelRO, GT, NF270, NF90, and GH membranes in solutions with pH values of 3 and 11

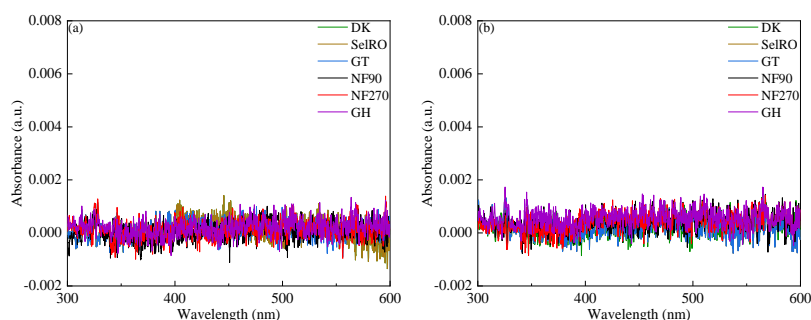


**Fig. S4** UV–Vis spectra of untreated DK, SelRO, GT, NF270, NF90, and GH membranes after immersion for 24 h in solutions with pH values of (a) 3 and (b) 11.

#### 6 Analyses on variance of densities of R-NH<sub>2</sub> and R-COOH measured at 12, 24, and 36 h

**Table S1** Analysis results of variance results ( $*p < 0.05$ )

Functional group	Time/h	$p$
R-NH <sub>2</sub>	12	0.998
	24	
	36	
R-COOH	12	0.927
	24	
	36	

## 7 Comparison of the dye adsorption method with the dye desorption method

**Table S2** Comparison of the dye adsorption method with the dye desorption method for density measurement of R-NH<sub>2</sub> and R-COOH

Functional group	Dye method	SD/(nmol·cm <sup>-2</sup> )	RSD/%	LOD/(μmol·L <sup>-1</sup> )	LOQ/(μmol·L <sup>-1</sup> )
R-NH <sub>2</sub>	Adsorption	0.011–0.024	2.25–5.40	0.0087	0.029
	Desorption	0.013–0.032	4.60–7.10	0.0188	0.062
R-COOH	Adsorption	0.007–0.022	2.56–3.58	0.0084	0.028
	Desorption	0.013–0.035	3.17–5.38	0.0110	0.037

Notes: SD, standard deviation; RSD, relative standard deviation; LOD, limit of detection; LOQ, limit of quantification.

## References

- [1] Lu D, Ma T, Lin S, et al. Constructing a selective blocked-nanolayer on nanofiltration membrane via surface-charge inversion for promoting Li<sup>+</sup> permselectivity over Mg<sup>2+</sup>. *Journal of Membrane Science*, 2021, 635: 119504
- [2] Yao X, Gonzales R R, Sasaki Y, et al. Surface modification of FO membrane for improving ammoniacal nitrogen (NH<sub>4</sub><sup>+</sup>-N) rejection: investigating the factors influencing NH<sub>4</sub><sup>+</sup>-N rejection. *Journal of Membrane Science*, 2022, 650: 120429
- [3] Coronell O, Benlto J M, Zhang X, et al. Quantification of functional groups and modeling of their ionization behavior in the active layer of FT30 reverse osmosis membrane. *Environmental Science & Technology*, 2008, 42: 5260–5266
- [4] Cao Y, Zhang H, Guo S, et al. A robust dually charged membrane prepared via catechol-amine chemistry for highly efficient dye/salt separation. *Journal of Membrane Science*, 2021, 629: 119287
- [5] Gegenschatz S A, Chiappini F A, Teglia C M, et al. Binding the gap between experiments, statistics, and method comparison: a tutorial for computing limits of detection and quantification in univariate calibration for complex samples. *Analytica Chimica Acta*, 2022, 1209: 339342
- [6] Li Q, Liu Y, Jia Y, et al. High performance Li<sup>+</sup>/Mg<sup>2+</sup> separation membrane by grafted short chain amino-rich monomers. *Journal of Membrane Science*, 2023, 677: 121634
- [7] Lu D, Ma T, Lin S, et al. Constructing a selective blocked-nanolayer on nanofiltration membrane via surface-charge inversion for promoting Li<sup>+</sup> permselectivity over Mg<sup>2+</sup>. *Journal of Membrane Science*, 2021, 635: 119504